A Design of Optimal Controller with Friction Reduction of Linear Motor-based Transfer System via Lift-force Control

*Jung Hyun Seo, **Jin Woo Lee, and ***Kwon Soon Lee

*, **, *** Dept. of Electrical Eng., Dong-A Univ., 840, Hadan 2-dong Saha-Gu Busan 604-714 Korea

(E-mail: *sanai3489@naver.com, **Jinwoo@donga.ac.kr, ***kslee@dau.ac.kr)

Abstract

A linear motor based transfer vehicle is significantly focused as transportation systems in marine terminals for the future. We propose a control method for the systems to hence mass reduction and propulsion effects at a starting point by using a lift-force mechanism. This method is newly based on a combined levitation-and-propulsion power by a lift and thrust force of a permanent magnet linear synchronous motor (PMLSM), which is carried out by a decoupled control. We exam that our proposed control largely compensates the vehicle weight, reduces friction effect of the system, and increases its velocity. Consequently, this result contributes numerous productivity and economical efficiency for the port systems.

Keywords: LMTT, PMLSM, Decoupled Control, Lift-force

1. Introduction

In recent years many technologies have been developed for port automate systems. An automated guided vehicle (AGV) is considered as one of the systems in the container yards. In general, an AGV involves various problems with difficulty and complexity for control, low speed and position accuracy, and heavy weight. Of them, however, the main one is about navigation which has difficulty to apply in a whole system and to work along with other systems. Recently, a LMTT transport system has been developed to overcome this difficulty. The LMTT is constructed using integration with linear motors and rail structures. Its main benefits include high force density and no need of sub-systems. Moreover, high accurate position control is realized from simple mechanical structures [1]. A traditional PMLSM vehicle which is mechanically supported by wheels generally uses only thrust force for propulsion. A large force which is produced simultaneously between PMs and stator iron yokes on the ground, is effectively rarely used. Apparently, this yields weight of the vehicle, which considerably increases its friction force between wheels and rails. In a new type of repulsive-controlled Maglev PMLSMs proposed by Yoshida [2]-[4], since a repulsive lift force simultaneously produces along with thrust forces, mass-reduced modes and the Maglev mode are realized by controlling the repulsive force. The purpose of using the lift force for mass reduction is not only for reducing the friction loss and wear of the wheel and rail, but also for applying it to the transfer operation of heavier goods beyond the rated transport capability.

This paper deals with fundamental LMTT, and proposes a concept of mass reduction and friction reduction for LMTT. The method is based on a new combined levitation-and-propulsion by lift and thrust forces of PMLSM which is carried out by the decoupled-control method proposed here. By applying thrust force and the repulsive lift force to the LMTT, a large rate of the vehicle weight is compensated, and it needs less thrust forces to propel the vehicle. When LMTT starts and reaches at workstation by a lift force, it reduces time consumption for arrival. And when it arrives at a target by an attractive force, it has shorter deceleration time. Thus, this possibly contributes much productivity and economical efficiency in the port systems.

2. LMTT(Linear Motor-based Transfer Technology)

2.1 Magnetic Force of PMLSM

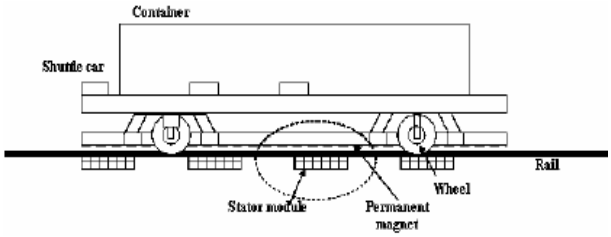

Figure 1. A LMTT vehicle system

The system consists of a substructure, shuttle cars, and a control system. If LMTT is used continuous stator, it causes rises of much cost. So, our proposed LMTT uses a discontinuous stator. Figure 1 shows scheme about LMTT suggested in this paper. The system is considered a permanent magnet linear synchronous motor consisted of stator modules on the rail and shuttle cars. Because of large variations of mover's weight by loading and unloading containers, differences among each characteristics for stator modules, stator module's defaults, and so on. LMTT is considered that the system is changed its model suddenly and variously.

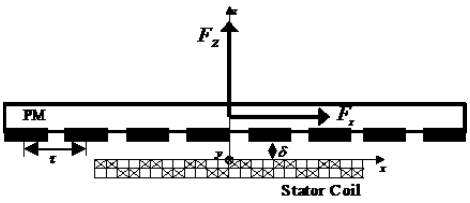

Figure 2. A structure of PMLSM

Figure 2 shows the longitudinal cross section of the stator PMLSM. The magnetic forces produced in the PMLSM can be resolved into three forces of thrust, lift, and lateral forces in a three-dimensional space coordinate. Because the vehicle is guided to run linearly on rollers and the guide-way in this paper, it is not necessary to take into account the effect of the lateral

force on the vehicle; here, we only take into account the thrust and lift forces. The transformation from the a-b-c reference frames to the d-q reference frames is defined as

$$\begin{bmatrix} d \\ q \end{bmatrix} = \sqrt{\frac{2}{3}} \begin{bmatrix} \cos\theta & \cos\left(\theta - \frac{2}{3}\pi\right) & \cos\left(\theta - \frac{4}{3}\pi\right) \\ -\sin\theta & -\sin\left(\theta - \frac{2}{3}\pi\right) & -\sin\left(\theta - \frac{4}{3}\pi\right) \end{bmatrix} \begin{bmatrix} a \\ b \\ c \end{bmatrix} \quad (1)$$

The machine model of a PMLSM can be described in synchronous rotating reference frame as follows:

$$v_q = R_s i_q + p\lambda_q + \omega_e \lambda_d \quad (2)$$

$$v_d = R_s i_s + p\lambda_d - \omega_e \lambda_q \quad (3)$$

Flux linkages for each axis, anguler velocities, and electric linear velocity are represented by

$$\lambda_q = L_q i_q \quad (4)$$

$$\lambda_d = L_d i_d + \lambda_{PM} \quad (5)$$

$$\omega_e = P\omega_r \quad (6)$$

Electromagnetic power is represented by

$$P_e = F_e v_e = 3P[\lambda_d i_q + (L_d - L_q) i_d i_q]\omega_e / 2 \quad (7)$$

Electromagnetic force is represented as

$$F_e = 3\pi P[\lambda_d i_q + (L_d - L_q) i_d i_q] / 2\tau \quad (8)$$

where

v_d, v_q	d-q axis voltages
i_d, i_q	d-q axis currents
R_s	winding resistance
L_d, L_q	d-q axis inductances
ω_r	angular velocity of the mover
ω_e	electrical anguler velocity
λ_{PM}	permanent magnet flux linkage
n_p	number of primary poles
p	differential operator
v	linear velocity of the mover

Thrust force can be described as

$$F_x = F_e = 3\pi\lambda_{PM} i_q / 2\tau \quad (9)$$

Simplified PMLSM drive system is able to describe as

$$F_e = K_t i_q^* \quad (10)$$

$$K_t = 3\pi n_p \lambda_{PM} / 2\tau \quad (11)$$

The normal force with air-gap g_0 can be described as

$$F_n = i_d \frac{\partial \lambda_d}{\partial g_0} + i_q \frac{\partial \lambda_q}{\partial g_0} \quad (12)$$

When the PM wave lags behind by mechanical load angle from the stator wave, an analytic formula of thrust force and lift force can be obtained as follows by solving the multi-boundary-value field problem using magnetic vector potential (MVP) transfer-matrix method [6]:

$$F_x = k_{F0}(\delta) I_1 \sin(\frac{\pi}{\tau} x_0) \quad (13)$$

$$F_Z = -k_{zS}(\delta) I_1^2 - k_{zMS}(\delta) I_1 \cos(\frac{\pi}{\tau} x_0) \quad (14)$$

where

k_{F0}, k_{zS}, k_{zMS}	:	coefficients for thrust and lift forces
I_1	:	effective armature current
τ	:	pole pitch
δ	:	air-gap length

$$I_1 = \sqrt{\frac{1}{2}(\frac{k_{zMS}}{k_{zS}})^2 - \frac{F_z}{k_{zS}} - \frac{k_{zMS}}{2k_{zS}} \sqrt{(\frac{k_{zMS}}{k_{zS}})^2 - 4(\frac{k_{zMS}}{k_{zS}} + \frac{F_x^2}{k_{F0}})}} \quad (15)$$

$$x_0 = \begin{cases} \sin^{-1}\dfrac{F_x}{k_{F0} I_1}, & I \neq 0,\ F_z \leq -k_{zS} I_1^2 \\ \tau - \sin^{-1}\dfrac{F_x}{k_{F0} I_1}, & I \neq 0,\ F_z > -k_{zS} I_1^2 \\ \textit{Arbitrary value}, & I = 0 \end{cases} \quad (16)$$

The first term on the right-hand side of (16) represents a magnetically attractive force between the current-carrying stator windings and the PM's yoke. The second term is the magnetic force component in the vertical direction, which is produced between the magnetic fields of PM and current-carrying stator windings.

2.2 Mathematical Modeling of Friction

Friction is an important aspect of many control systems both for high quality servo mechanisms and hydraulic systems. The linear motion servo system with nonlinear friction and variation of mover's mass can be shown as figure 3.

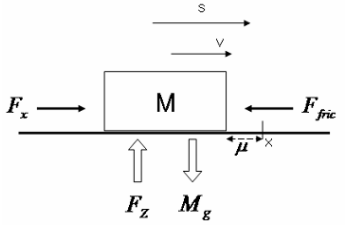

Figure 3. Configuration of the considered system and each component.

$$M\frac{d^2x}{dt^2} = u - F \quad (17)$$

where

x	mover position
M	mass
u	control input(thrust force)
F	friction force.

LuGre dynamic friction model F is considered the model of bristles reaction between two surfaces [7]. And it based on the average deflection behaviour of the elastic bristles. It can be described by equation (18).

$$F = \sigma_0 z + \sigma_1 \frac{dz}{dt} + \sigma_2 v \tag{18}$$

where,

z	average deflection of elastic bristles.
v	mover's velocity
σ_0	coefficient of stiffness
σ_1	damping coefficient
σ_2	coefficient of viscous.

The equation of bristle deflection z and the positive definite function that relies on factors such as surface material characteristics can be described by equations (19) and equations (20) is a parameterization of g that has been proposed to describe by the Stribeck effect[8].

$$\frac{dz}{dt} = v - \frac{\sigma_0 |v|}{g(v)} z \tag{19}$$

$$g(v) = F_C + (F_S - F_C) e^{-(v/v_s)^2} \tag{20}$$

where,

F_C	Coulomb friction level
F_S	stiction force level
v_s	Stribeck velocity.

In this paper, it needs to modify equation (19) for considering the mass and the normal force variation system as follows:

$$\frac{dz}{dt} = v - \theta \frac{\sigma_0 |v|}{g(v)} z \tag{21}$$

where, θ is an uncertain friction scale factor that is normalized by the initial mass $M(0)$. Therefore, the relationship between the actual variation of mass and θ can be noted as follows:

$$\theta(t) = \frac{M(0)}{M(t)} \tag{22}$$

In case use the levitation force, the LMTT's weight change for vertical axis. And the estimated LMTT's weight is can be described as equation (23).

$$\hat{M}(t, F_Z) = M(t) - \mu_{scale}(F_Z / g) \tag{23}$$

And, equation (21) can be described like equation (24).

$$\frac{dz}{dt} = v - \left(\frac{M(0)}{\hat{M}(t, F_Z)} \frac{\sigma_0 |v|}{g(v)} z \right) \tag{24}$$

The model given by (19) and (20) is characterized by the function g and the parameters σ_0, σ_1, σ_2. The function $\sigma_0 g(v) + \sigma_2 v$ can be determined by meaning the steady-state friction force when the velocity is held constant. It follows from equation (20) that for steady-state motion the relation between velocity and friction force is given by [9].

$$\begin{aligned} F \approx F_{SS} &= g(v)\,\mathrm{sgn}(v) + \sigma_2 v \\ &= \{F_C + (F_S - F_C) e^{-(v/v_s)^2}\}\,\mathrm{sgn}(v) + \sigma_2 v \end{aligned} \tag{25}$$

Note, however, that when velocity is not constant, the dynamic of the model will be very important and give rise to different type of phenomena.

2.3 Design of Control System

In the paper, the structure of control system is composed of PM-LSM having two input that normal force and thrust force show like as the figure 4. The proposed control system is decoupled-control method, and the method is based on a new combined levitation and propulsion due to lift and thrust force of linear synchronous motor and can be carried out by the decoupled-control proposed [10].

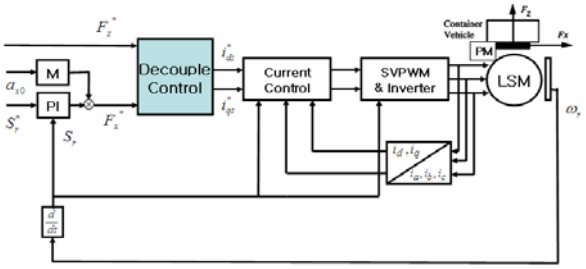

Figure 4. Proposed PM-LSM drive system

According to the optimal servo-control theory and the minimum error control method shown in the figure 5.

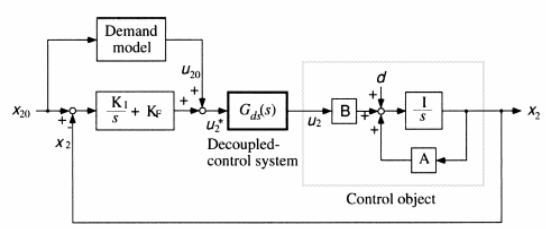

Figure 5. Control system diagram

The demand force F_x^*, F_z^* can be deduced as follows:

$$F_x^* = k_{xP}(x_{20} - x_2) + k_{xD}(v_{x20} - v_{x2}) + k_{xI} \int (x_{20} - x_2) dt \tag{26}$$

$$F_z^* = k_{zP}(z_{20} - z_2) + k_{zD}(v_{z20} - v_{z2}) + k_{zI} \int (z_{20} - z_2) dt \tag{27}$$

where,

x_{20}, x_2	demand and measured positions,
v_{x20}, v_{x2}	demand and measured speeds,
z_{20}, z_2	demand and measured positions of levitation,

v_{z20}, v_{z2} demand and measured speeds of levitation,
k_{xP}, k_{xD} feedback gains for propulsion,
k_{zP}, k_{zD} feedback gain for levitation,
k_{xI}, k_{zI} integral gain for propulsion and levitation.

And we have turned PID's coefficient by ES as follow,

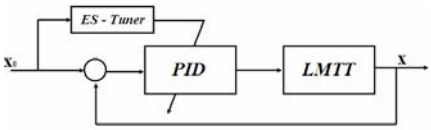

Figure 6. ES-turned PID Control system diagram

3. Simulation and Results

According to the control principle proposed above, the motion of levitation and propulsion of LMTT are simulated. The scenario is as follows:

We assumed factors to Shuttle Car and Container's weight is 60 [ton], maximum thrust force is 25 [kN], coefficient of friction is 1% of total weight, and accuracy is ±3 [mm]. I use decoupled control by ES-turned and have simulated shuttle car's moving distance 20, 50, 100, 150[m]. I have compared using lift-force with no. I have used lift-force that used time is 2 [sec], and force is half the size of a total mass. The result data is as follow,

Table 1. Arrival time using Lift Force

Distance[m] \ Lift Force	30[KN]	0[KN]
20	7.1[sec]	8.8[sec]
50	9.8[sec]	11.8[sec]
100	15.6[sec]	17.4[sec]
150	20.4[sec]	22.7[sec]

In table 1 is shown a movement distance of LMTT is far. We show arrival time reduced. And according to decoupled control simulation I have limited to maximum energy in LMTT by mechanical character, according to decoupled control simulation result is represented by the figure 7,

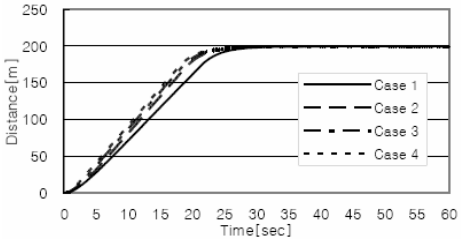

Figure 7. The distance variation for the restrained input energy (200[m])

Table 2. The distance variation for the restrained input energy

Case	Thrust[kN]	Lift[kN]	Time of Arrival [sec]		
			100m	3m	0m
1	250	0	7.7	28.1	32.1
2	240	100	7.0	26.0	30.4
3	230	200	6.4	25.4	30.4
4	220	300	6.0	25.0	31.5

The main data of simulation are listed in table 2. The table 2 show LMTT's performance improvement using lift-force in same energy. This is PMLSM's characteristic that a stator has two force, thrust and lift-force. And it is more powerful lift-force than any linear motors. LMTT raised the efficiency of system by using lift-force and efficient distribution. Case 2, 3, and 4 are improved 5.3[%], 5.3[%], and 1.9[%] better than case 1. In the results, the best chose is case 4, because it is Time of Arrival of 100[m], 3[m] to target better than other cases.

And the following simulations show efficiency improved of system by ES-Tuned Control better than. Using scenario is as follow, The lift force is 30[ton], maximum thrust is 250[kN], mass is 60[ton], demand distance is 200[m].

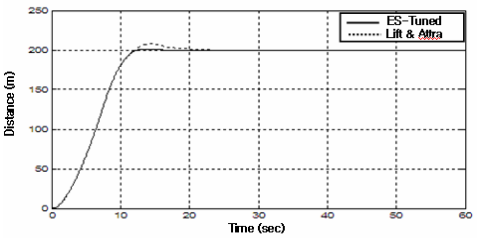

Figure 8. Distance(m)

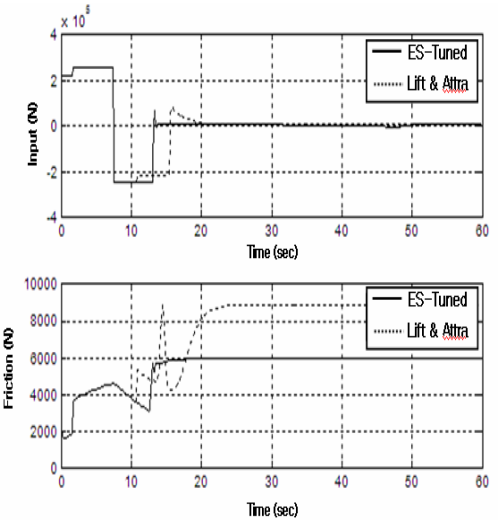

Figure 9. Input(N) and Friction(N)

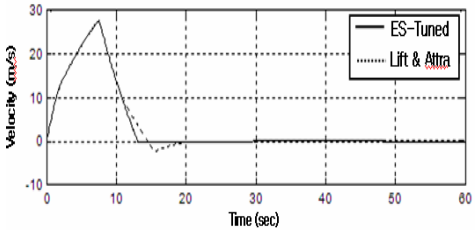

Figure 10. Velocity(m/s)

Above simulation result show system by using ES-Tunning is improved for distance, friction, velocity.

4. Conclusions

In this paper, we proposed LMTT is used lift-force. And I show usefulness of lift-force by simulation. It appeared clearly that the effectiveness of lift-force is movement long distance better than short.

And proposed decoupled control mode with lift-force and propulsion control is very useful in practical application, from the viewpoint of less friction loss, less wear, less air pollution, less noise, and less maintenance cost. It is possible to increase greatly the payload by using this new transport approach.

In this paper, we demonstrated a proposed theory only simulation. But lift-force will have to be using precise controller better than ES-tuned in the future.

Acknowledgement

The work was supposed by the National Research Laboratory (NRL) program of the Korean Ministry of Science and Technology (MOST).

References

[1] E. Huth, W. Canders, and H. Mosebach, “Linear motor transfer technology for container terminals,” in *Proc. LDIA’98*, Tokyo, Japan, 1998, pp. 39–41.

[2] K. Yoshida, “Linear synchronous motor propulsion method for guided vehicle,” Japanese Patent Pub. 1991-27730.

[3] K. Yoshida, H. Takami, X. Kong, and A. Sonoda, "Mass Reduction and Propulsion Control for a Permanent-Magnet Linear Synchronous Motor Vehicle", *IEEE Trans. on Industry Applications*, Vol. 37, No. 1, 2001, pp. 67-72.

[4] K. Yoshida, X. Kong, and H. Takami, “Network Transport Automation Study of PM LSM Vehicle on Orthogonally-Switching-Guideway”, *Industry Applications Conference*, Vol. 2, 2000, pp. 1109-1114.

[5] F. J. Lin, C. H. Lin, and C. M. Hong, “Robust Control of Linear Synchronous Motor Servodrive using Disturbance Observer and Recurrent Neural Network Compensator,” *IEEE Proc. of Electrical Power Applications*, Vol. 147, No. 4, 2000, pp. 263-272.

[6] K. Yoshida and H. Weh, “Method of modeling permanent magnet for analytical approach to electrical machinery,” *Arch. Elektrotech.*, 1985, vol. 68, no. 4, pp. 229–239.

[7] Klaus-Peter Franke, “Boosting Efficiency of Split Marine Container Terminals by Innovative Technology”, *Proc. of IEEE Int. Conf. on Intelligent Transportation Systems*, 2001, pp. 774-779.

[8] F. J. Lin, R. J. Wai, and C. M. Hong, “Hybrid Supervisory Control Using Recurrent Fuzzy Neural Network for Tracking Periodic Inputs”, *IEEE Trans. on Neural Networks*, Vol. 12, No. 1, January, 2002.

[9] Rong-Jong Wai, Faa-Jeng Lin, “Adaptive Recurrent-Neural-Network Control for Linear Induction Motor”, *IEEE Trans. on Aerospace & Electronic Systems*, Vol. 37, No. 4, 2001, pp. 1176-1192.

[10] M. A. Rahman, “Analysis of Current Controllers for Voltage Source Inverter”, *IEEE Trans. On Industrial Electronics*, Vol. 44, No. 4, 1997, PP. 477-485.